Nrf2 and PGC-1α signaling in temozolomide resistance in glioblastoma under hypoxia

PINPAT TRIPATARA[1*], TASANEE ONKOKSOONG[1*], SUNISA PRASOPPORN[1,2], SITH SATHORNSUMETEE[3], SIWANON JIRAWATNOTAI[1,2] and URAIWAN PANICH[1]

[1]Department of Pharmacology, Faculty of Medicine, Siriraj Hospital, Mahidol University, Bangkok 10700, Thailand; [2]Siriraj Center of Research Excellence for Systems Pharmacology, Department of Pharmacology, Faculty of Medicine, Siriraj Hospital, Mahidol University, Bangkok 10700, Thailand; [3]Department of Medicine, Faculty of Medicine, Siriraj Hospital, Mahidol University, Bangkok 10700, Thailand

Received February 2, 2026; Accepted August 6, 2026

DOI: 10.3892/br.2026.2202

Abstract. Hypoxia is a key contributor to chemoresistance in glioblastoma (GBM), partly through the activation of nuclear factor erythroid 2-related factor 2 (Nrf2)-dependent cellular stress responses and mitochondrial adaptive programs. The present study investigated Nrf2 signaling in hypoxia-associated resistance to temozolomide (TMZ) in U87MG cells, a glioblastoma cell line, and evaluated whether pharmacological suppression of Nrf2 pathway output with brusatol enhances TMZ sensitivity under hypoxic conditions. U87MG cells were cultured under normoxic or hypoxic conditions (1% O_2) and treated with TMZ, brusatol, or their combination. DAPI-based cell-counting assays were used to determine half-maximal inhibitory concentrations (IC_{50} values) and assess drug interactions by combination index analysis. Hypoxia-inducible factor 1α (HIF-1α) expression, epidermal growth factor receptor (EGFR) phosphorylation and Nrf2 nuclear accumulation were analyzed by western blotting. The expression of antioxidant and growth factor-related signaling genes and downstream targets of peroxisome proliferator-activated receptor gamma coactivator 1α (PGC-1α), a key regulator of mitochondrial bioenergetics, was quantified by real-time PCR (qPCR). PGC-1α subcellular localization and oxidative DNA damage, assessed using 8-hydroxy-2'-deoxyguanosine, were evaluated by immunofluorescence. Hypoxia markedly increased the TMZ IC_{50} and was accompanied by elevated HIF-1α expression and enhanced Nrf2 nuclear accumulation. Combination index analysis identified synergistic interactions between TMZ and brusatol under normoxia, whereas no synergistic interaction was detected under hypoxia; nonetheless, brusatol still enhanced TMZ sensitivity under hypoxia based on direct cell-count analysis. Hypoxia markedly upregulated antioxidant genes (GCLM, GPX1, GSTP1, HO-1, NQO1 and SOD1) and growth- and survival-related genes (NF-κB, TGF-β, EGF and EGFR) and induced a PGC-1α-associated mitochondrial transcriptional program, as evidenced by increased expression of sirtuin 3, cytochrome *c* and ATP synthase F1 subunit β. Co-treatment with TMZ and brusatol suppressed antioxidant gene expression, reduced EGFR phosphorylation, attenuated PGC-1α-linked mitochondrial gene expression, and increased oxidative DNA damage. These findings indicated that pharmacological suppression of Nrf2 pathway output by brusatol was associated with enhanced TMZ sensitivity under hypoxic conditions in U87MG cells, together with reduced antioxidant gene expression, lower EGFR phosphorylation, attenuation of PGC-1α-associated mitochondrial responses, and increased oxidative DNA damage in GBM, potentially reflecting suppression of HIF-1α-dependent as well as Nrf2-dependent signaling.

Correspondence to: Professor Uraiwan Panich, Department of Pharmacology, Faculty of Medicine, Siriraj Hospital, Mahidol University, 2 Wanlang Road, Bangkoknoi, Bangkok 10700, Thailand
E-mail: uraiwan.pan@mahidol.ac.th

*Contributed equally

Abbreviations: 8-OHdG, 8-hydroxy-2'-deoxyguanosine; ATP5F1B, ATP synthase F1 subunit β; CI, combination index; CYCS, cytochrome c; DCFH-DA, 2',7'-dichlorodihydrofluorescein diacetate; EGF, epidermal growth factor; EGFR, epidermal growth factor receptor; GBM, glioblastoma; GCLM, glutamate-cysteine ligase modifier subunit; GPX1, glutathione peroxidase 1; GSTP1, glutathione S-transferase pi 1; HIF-1α, hypoxia-inducible factor 1 alpha; HO-1, heme oxygenase 1; NF-κB, nuclear factor κB; SOD1, superoxide dismutase 1; IC_{50}, half-maximal inhibitory concentration; PGC-1α, peroxisome proliferator-activated receptor gamma coactivator 1 alpha; qPCR, quantitative polymerase chain reaction; ROS, reactive oxygen species; SIRT3, sirtuin 3; TBP, TATA-binding protein; TGF-β, transforming growth factor beta; TMZ, temozolomide

Key words: brusatol, chemoresistance, glioblastoma, hypoxia, nuclear factor erythroid 2-related factor 2, peroxisome proliferator-activated receptor γ coactivator 1 α

Introduction

Glioblastoma (GBM) is the most common primary malignant brain tumor and is highly aggressive in adults. Standard therapy combines maximal safe resection with radiotherapy and concomitant and adjuvant temozolomide (TMZ) (1-3). Rapidly proliferating solid tumors, including GBM, frequently

develop hypoxic niches associated with poor prognosis and therapeutic failure (4,5). Tumor hypoxia has been implicated in TMZ resistance and GBM recurrence (6,7). Hypoxia promotes GBM cell adaptation through coordinated activation of hypoxia-inducible factor (HIF) programs and reinforcement of EGFR signaling, including the EGFR-PI3K/AKT pathway (4,8). Hypoxia also perturbs mitochondrial electron transport and redox balance, generating reactive oxygen species (ROS) signals that can contribute to HIF-1α stabilization and transcriptional reprogramming (9-11). Under normoxia, HIF-1α is hydroxylated by prolyl hydroxylases, promoting von Hippel-Lindau (VHL)-dependent ubiquitination and proteasomal degradation. Under hypoxia, reduced prolyl hydroxylation impairs VHL recognition, allowing HIF-1α stabilization and transcriptional activation (12,13). In parallel, Nrf2 is normally bound by Kelch-like ECH-associated protein 1 (Keap1), which acts as a substrate adaptor for the CUL3-RBX1 E3 ubiquitin ligase complex and promotes Nrf2 ubiquitination and proteasomal degradation. Hypoxia-associated oxidative stress may modify redox-sensitive cysteine residues in Keap1, thereby impairing Keap1-dependent Nrf2 ubiquitination and promoting Nrf2 stabilization and nuclear accumulation (14,15). Nrf2 is a central transcription factor that regulates antioxidant and cytoprotective genes, thereby limiting oxidative and electrophilic stress. In cancer, however, Nrf2 can be co-opted to support survival and treatment resistance; in GBM models, Nrf2 depletion suppresses hypoxia-driven angiogenic signaling and sensitizes glioma cells to stress and therapy under hypoxic conditions (16-18). Nrf2 also intersects with mitochondrial metabolism and emerging evidence links Nrf2 activity to PGC-1α-associated transcriptional programs that can support oxidative metabolism and therapy tolerance (19,20). However, how Nrf2-dependent stress responses interface with PGC-1α-linked mitochondrial transcriptional programs during hypoxia-associated TMZ resistance in GBM remains unclear. Brusatol was originally reported to suppress Nrf2 signaling and sensitize cancer cells to chemotherapy by rapidly decreasing Nrf2 protein abundance and Nrf2-dependent transcription (21). Subsequent mechanistic work indicates that brusatol acts primarily as a broad inhibitor of protein translation, causing transient depletion of short-lived proteins such as Nrf2; therefore, brusatol is interpreted here as a tool for suppressing Nrf2 pathway output with known off-target liabilities (22,23). The present study investigated whether hypoxia-associated Nrf2 activation accompanies TMZ resistance and whether pharmacological suppression of Nrf2 pathway output with brusatol enhances TMZ sensitivity. The present study focused on EGFR signaling, redox homeostasis, and PGC-1α-linked mitochondrial transcriptional programs to evaluate the potential of combining suppression of Nrf2 pathway output with standard TMZ chemotherapy in hypoxic GBM cells.

Materials and methods

Cell culture and treatment. U87MG cells (cat. no. HTB-14™; ATCC), a glioblastoma cell line of unknown origin, and U138MG cells (cat. no. HTB-16™; ATCC), a human glioblastoma cell line, were obtained from the American Type Culture Collection. The two cell lines were cultured in DMEM (cat. no. 12800017; Invitrogen; Thermo Fisher Scientific, Inc.) supplemented with 10% fetal bovine serum (cat. no. A5256701; Invitrogen; Thermo Fisher Scientific, Inc.), 100 U/ml penicillin G (cat. no. P3032; MilliporeSigma), and 100 μg/ml streptomycin (cat. no. S9137; MilliporeSigma) at 37˚C in a humidified atmosphere containing 5% CO_2/95% air. Cell line authentication by STR profiling was not performed in the present study, representing a limitation of the experimental design.

Hypoxic conditions. Cells were placed in a tightly sealed hypoxia chamber (cat. no. 27310; STEMCELL Technologies). The chamber was flushed at 2.0 l/min for 5 min with a gas mixture containing 1% O_2, 5% CO_2 and N_2 as the balance gas (Polysource Co., Ltd.) (24). The inlet and outlet valves were then closed, and the chamber was placed in a CO_2 incubator for the indicated durations (that is, 24, 48 or 72 h).

DAPI-based cell-counting assay. Cells were seeded in 96-well plates (cat. no. 3603; Corning) at a density of 10,000 cells/well and allowed to attach for 24 h. Cells were then treated with TMZ alone (3-300 μM; cat. no. HY-17364; MedChemExpress), brusatol alone (7.5-120 nM; cat. no. SML1868; MilliporeSigma), or combinations of brusatol (7.5, 15.0, 30 and 60 nM) and TMZ (3, 10, 30 and 90 μM) for 72 h under hypoxic (1% O_2) or normoxic (21% O_2) conditions. Cells were fixed with 4% paraformaldehyde at 37˚C for 15 min, washed twice with phosphate-buffered saline (PBS), and stained with 1 μg/ml DAPI (cat. no. D9542; MilliporeSigma) in PBS for 30 min at room temperature. Cells were counted using an Operetta High-Content Imaging System and Harmony analysis software (Revvity, Inc.). Cell numbers were expressed as percentages of the untreated control. The IC_{50} values of TMZ and brusatol in U87MG cells were calculated using GraphPad Prism (Dotmatics). Drug interactions were evaluated using the combination index (CI), calculated from concentration-effect data with CompuSyn software version 1.0 (ComboSyn, Inc.). CI<1 indicated synergism, CI=1 indicates an additive effect, and CI>1 indicates antagonism, as previously described (25).

Measurement of intracellular ROS by flow cytometry. Cells were exposed to hypoxia for 2, 4, 8, 16, or 24 h. The medium was removed, and cells were incubated with 5 μM 2',7'-dichlorodihydrofluorescein diacetate (DCFH-DA; cat. no. D6883; MilliporeSigma) in PBS at 37˚C for 30 min, as previously described (26). The stained cells were immediately analyzed using a CytoFLEX flow cytometer (Beckman Coulter, Inc.). Flow cytometry data were analyzed using FlowJo Software version 10 (BD Life Sciences). Data were expressed as percentages of the normoxic control (set to 100%).

Western blotting of HIF-1α expression and Nrf2 nuclear localization. Cells were exposed to hypoxia for the indicated durations (4-24 h). Total cellular protein was extracted using cell lysis buffer containing 0.1% NP-40, 150 mM NaCl, 50 mM Tris-HCl (pH 8.0) and protease inhibitor cocktail and cytosolic and nuclear fractions were prepared using a Nuclear Extraction kit (cat. no. ab113474; Abcam), as previously described (26). Protein concentrations were determined using Bradford assay. A total of 50 μg protein per lane was

separated by 10% sodium dodecyl sulfate-polyacrylamide gel electrophoresis and transferred to polyvinylidene difluoride membranes (Bio-Rad Laboratories, Inc.). The membranes were washed with PBS containing 0.1% Tween-20 (PBST) and blocked with 5% non-fat dry milk in PBST for 1.5 h at room temperature. The membranes were incubated with the following primary antibodies for 18 h at 4˚C: Anti-Nrf2 (1:500; cat. no. ab137550; Abcam; 110 kDa), anti-HIF-1α (1:500; cat. no. ab1; Abcam; 92 kDa), anti-EGFR (1:5,000; cat. no. ab52894; Abcam; 175 kDa), anti-phosphorylated (p-)EGFR (Y1068; 1:1,000; cat. no. ab40815; Abcam; 175 kDa), anti-β-actin (1:5,000; cat. no. ab8227; Abcam; 42 kDa), and anti-TATA-binding protein (TBP; 1:500; cat. no. ab818; Abcam; 38 kDa). Appropriate horseradish peroxidase-conjugated secondary antibodies (Abcam; 1:5,000) were incubated for 1.5 h at room temperature. Protein bands were detected using Clarity Western ECL Blotting Substrate (cat. no. 1705062; Bio-Rad Laboratories, Inc.) and visualized with a VersaDoc 4000 MP Imaging System (Bio-Rad Laboratories, Inc.). Band densities were quantified using ImageJ version 1.47 (National Institutes of Health). Protein levels were normalized to β-actin for whole-cell and cytosolic fractions and to TBP for nuclear fractions. Phospho-EGFR and total EGFR levels were first normalized to β-actin, after which the phospho-EGFR/total EGFR ratio was calculated. Data were expressed as fold changes relative to normoxic control cells.

mRNA quantification by reverse transcription-quantitative (RT-q) PCR. Cells were seeded in 6-well plates at a density of 100,000 cells/well and allowed to attach for 24 h. Total RNA was extracted using a Total RNA Extraction Kit (cat. no. RBD050; Geneaid Biotech Ltd.) according to the manufacturer's protocol. cDNA was synthesized using an iScript™ cDNA Synthesis Kit (cat. no. 1708891; Bio-Rad Laboratories, Inc.) according to the manufacturer's protocol. Primer sequences were designed using Primer Express version 3.0 software (Applied Biosystems; Thermo Fisher Scientific, Inc.) and are listed in Table SI. qPCR was performed using a KAPA SYBR® FAST qPCR kit (cat. no. KM4102; Kapa Biosystems). Thermocycling conditions were as follows: Initial denaturation (enzyme activation) for 3 min at 95˚C, followed by 40 cycles of denaturation for 3 sec at 95˚C and annealing for 30 sec at 60˚C. Following amplification, dissociation (melt-curve) analysis was performed at 95˚C for 1 sec, 60˚C for 1 sec and 95˚C for 1 sec. Relative mRNA expression levels were calculated using the 2-ΔΔCq method (27), with β-actin as the internal reference gene. qPCR and data analysis were performed as previously described (28). Experiments were performed using ≥3 independent biological replicates.

Immunofluorescence assay. U87MG cells were seeded in cellcarrier-96 Ultra plate (cat. no. 6055300; Revvity, Inc.) at a density of 100,000 cells/well and allowed to attach for 24 h. Cells were treated with 10 μM TMZ and/or 15 nM brusatol at 37˚C under normoxic or hypoxic conditions for 24 h. U87MG cells were fixed with 4% paraformaldehyde for 10 min at room temperature and washed twice with ice-cold PBS. Cells were permeabilized with cold methanol for 10 min and washed with PBST. Non-specific binding was blocked with Odyssey Blocking Buffer (cat. no. 927-70001; LI-COR Biosciences) for 1 h at room temperature. Cells were incubated overnight at 4˚C with primary antibodies against PGC-1α (cat. no. ab191838; Abcam; 1:500) and 8-hydroxy-2'-deoxyguanosine (8-OHdG; cat. no. sc-66036; Santa Cruz Biotechnology, Inc.; 1:500). After four washes with PBST, cells were incubated for 1 h at room temperature with Alexa Fluor® 647-conjugated goat anti-mouse IgG (cat. no. ab150115; Abcam; 1:500) or goat anti-rabbit IgG (cat. no. ab150083; Abcam; 1:500). Cells were then washed twice with PBST and once with PBS. Nuclei were counterstained with DAPI (cat. no. D9542; MilliporeSigma) for 30 min at room temperature and washed three times with PBS. Images were acquired using an Operetta CLS High-Content Imaging System (Revvity, Inc.) with a 40x objective (DAPI: excitation, 350 nm; emission, 470 nm; Alexa Fluor 647: excitation, 650 nm; emission, 665 nm) and analyzed using Columbus software (Revvity, Inc.). PGC-1α translocation was quantified by fluorescence-intensity analysis. Nuclear regions were defined using DAPI fluorescence, and cytoplasmic regions were generated by expanding the nuclear boundary by 10 pixels. Mean fluorescence intensities in the nucleus (N) and cytoplasm (C) were measured, and nuclear translocation was expressed as the N/C ratio. Whole-cell fluorescence intensity was calculated as the mean of the N and C intensities, (N + C)/2. All measurements were background-corrected using the mean pixel intensity from blank wells and normalized to the mean value of the normoxic control (29).

Statistical analysis. Data are presented as the mean ± SD from at least three independent biological replicates (n≥3). Statistical analyses were performed using GraphPad Prism version 9.0.0 (Dotmatics). Comparisons between two groups were performed using unpaired two-tailed Student's t-tests. Experiments involving more than two groups were analyzed by one-way ANOVA followed by Dunnett's post hoc test against the relevant control. For matched-dose comparisons across a dose-response series (e.g., TMZ alone vs. TMZ plus brusatol at each TMZ concentration), unpaired two-tailed t-tests were used, as specified in the figure legends. Formal assessments of normality and homogeneity of variance were not performed prior to statistical analysis, which should be considered a limitation of the study. $P<0.05$ was considered to indicate a statistically significant difference.

Results

Hypoxia reduces TMZ sensitivity in U87MG cells. To evaluate the effects of hypoxia on glioblastoma cell proliferation, U87MG and U138MG cells were exposed to 1% O_2 for 24, 48, or 72 h. In U87MG cells, hypoxia markedly increased cell proliferation after 72 h compared with normoxia (21% O_2; P=0.017; Fig. 1A). U87MG cells also showed reduced TMZ sensitivity under hypoxia, as indicated by an increase in the TMZ IC_{50} from 141.5±25.0 μM under normoxia to 267.0±45.0 μM under hypoxia (Fig. 1B). By contrast, the brusatol IC_{50} values were similar under normoxia and hypoxia (38.8±6.9 and 42.8±8.4 nM, respectively; Fig. 1C). In U138MG cells, hypoxia markedly increased cell proliferation after 72 h compared with normoxia (P=0.009; Fig. 1D). However, the TMZ and brusatol dose-response profiles were similar under

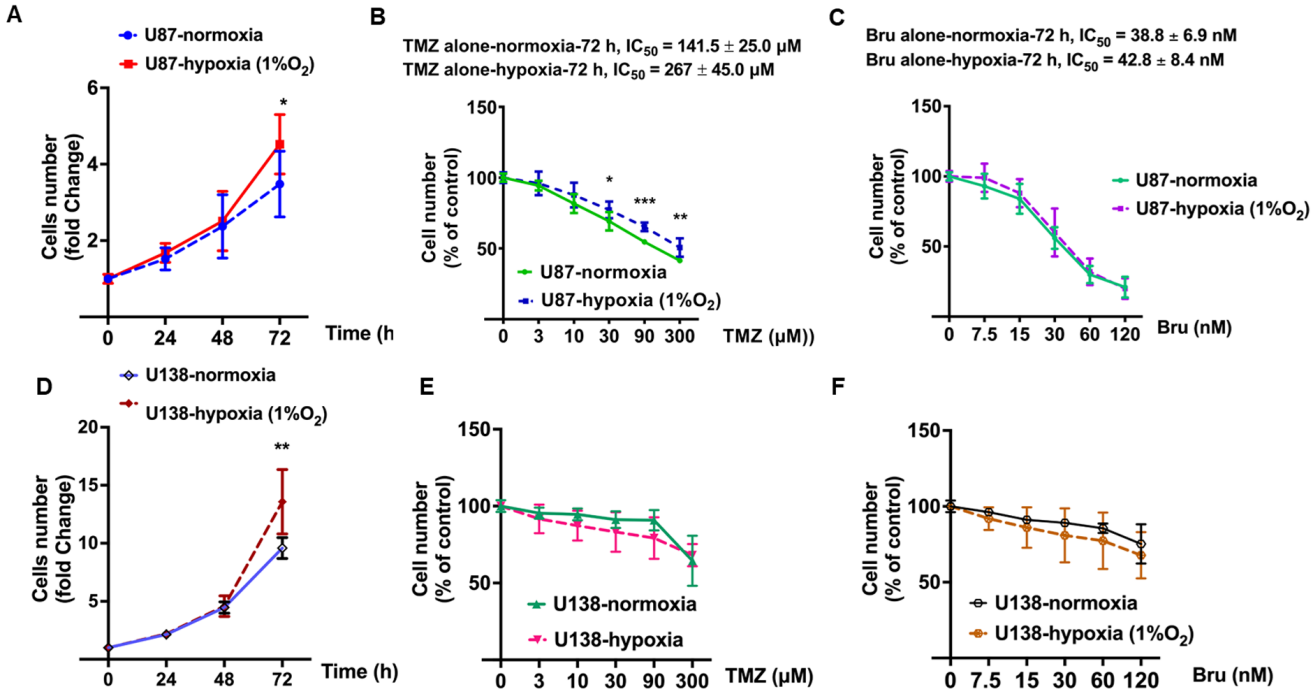

Figure 1. Effects of TMZ and Bru on relative cell number in U87MG and U138MG cells under normoxia and hypoxia. (A) U87MG cell proliferation under normoxia (21% O_2) or hypoxia (1% O_2) for up to 72 h. Dose-response curves for (B) TMZ (3-300 μM) and (C) Bru (7.5-120 nM). (D) U138MG cell proliferation under normoxia or hypoxia for up to 72 h. Dose-response curves for (E) TMZ and (F) Bru after 72 h under normoxia or hypoxia, assessed by DAPI-based cell counting. Data are presented as the mean ± SD (n≥3). Differences between normoxia and hypoxia at each time point or matched concentration were evaluated using unpaired two-tailed Student's t-test. *P<0.05, **P<0.01, and ***P<0.001 vs. normoxia. TMZ, temozolomide; Bru, brusatol.

normoxic and hypoxic conditions (Fig. 1E-F). Consistent with these findings, hypoxia produced only a slight reduction in the p-EGFR/EGFR ratio, and co-treatment with TMZ and brusatol did not markedly alter EGFR phosphorylation relative to TMZ alone under either oxygen condition (Fig. S1). As U138MG cells did not exhibit a hypoxia-dependent shift in treatment response, subsequent mechanistic experiments were performed in U87MG cells, which displayed a distinct hypoxia-associated TMZ-resistant phenotype.

Hypoxia induces HIF-1α and upregulates Nrf2 signaling and target gene expression. Western blotting revealed time-dependent induction of HIF-1α in U87MG cells after 4, 8 and 16 h of hypoxia (Fig. 2A). Nrf2 nuclear accumulation was markedly enhanced after 16 h, as indicated by the nuclear-to-cytosolic (N/C) Nrf2 ratio and the nuclear and cytosolic Nrf2 measurements (Fig. 2B-E). Total Nrf2 immunoreactivity in the expected molecular-weight region (100-130 kDa) was also elevated after 8 h hypoxia (Fig. 2F). Nrf2 mRNA expression was markedly upregulated after 4 h of hypoxia (P<0.001; Fig. 2G). Because hypoxia can remodel redox balance and engage stress-response pathways, including HIF-1α and Nrf2 (15,30), intracellular ROS levels were measured over time. ROS increased transiently at 2 h and then decreased below normoxic control levels at 8 and 16 h (Fig. 2H-I), during the period of increased Nrf2 signaling. Hypoxia also increased the expression of the Nrf2 target genes GSTP1 and NQO1, with peak expression at 18 h (Fig. S2).

Brusatol, a pharmacological suppressor of Nrf2 pathway output, sensitizes U87MG cells to TMZ. Given the hypoxia-associated increase in Nrf2 signaling, the present study examined whether pharmacological suppression of Nrf2 pathway output with brusatol could enhance TMZ sensitivity. The brusatol concentrations used (7.5-120 nM) were selected based on published evidence of Nrf2 pathway suppression and chemosensitization at low nanomolar concentrations in cancer models, including GBM (21,22,31). DAPI-based cell counting showed that co-treatment with TMZ and brusatol markedly reduced U87MG cell numbers compared with TMZ alone under both normoxic and hypoxic conditions (Fig. 3A and B). Combination index analysis indicated synergistic interactions that were more pronounced under normoxia (Fig. 3C). Under hypoxia, no synergistic interaction was detected by CI analysis (Fig. 3D), although brusatol still enhanced TMZ sensitivity at several dose combinations based on direct cell-count analysis (Fig. 3B).

Brusatol-enhanced TMZ sensitivity is associated with reduced EGFR phosphorylation. To investigate mechanisms associated with brusatol-enhanced TMZ sensitivity, the present study examined antioxidant and growth factor-related gene expression under hypoxia. Hypoxia markedly upregulated several antioxidant genes (GCLM, GPX1, GSTP1, HO-1, NQO1 and SOD1) (32,33), as well as genes associated with cell survival and proliferation, including NF-κB, TGF-β, EGF and EGFR (32-34) (Fig. 4A). Co-treatment with TMZ and brusatol markedly decreased the hypoxia-induced expression of antioxidant genes and EGFR relative to TMZ alone, whereas NF-κB and TGF-β expression remained largely unchanged (Fig. 4B). Under normoxia, combined treatment with TMZ and brusatol did not markedly alter

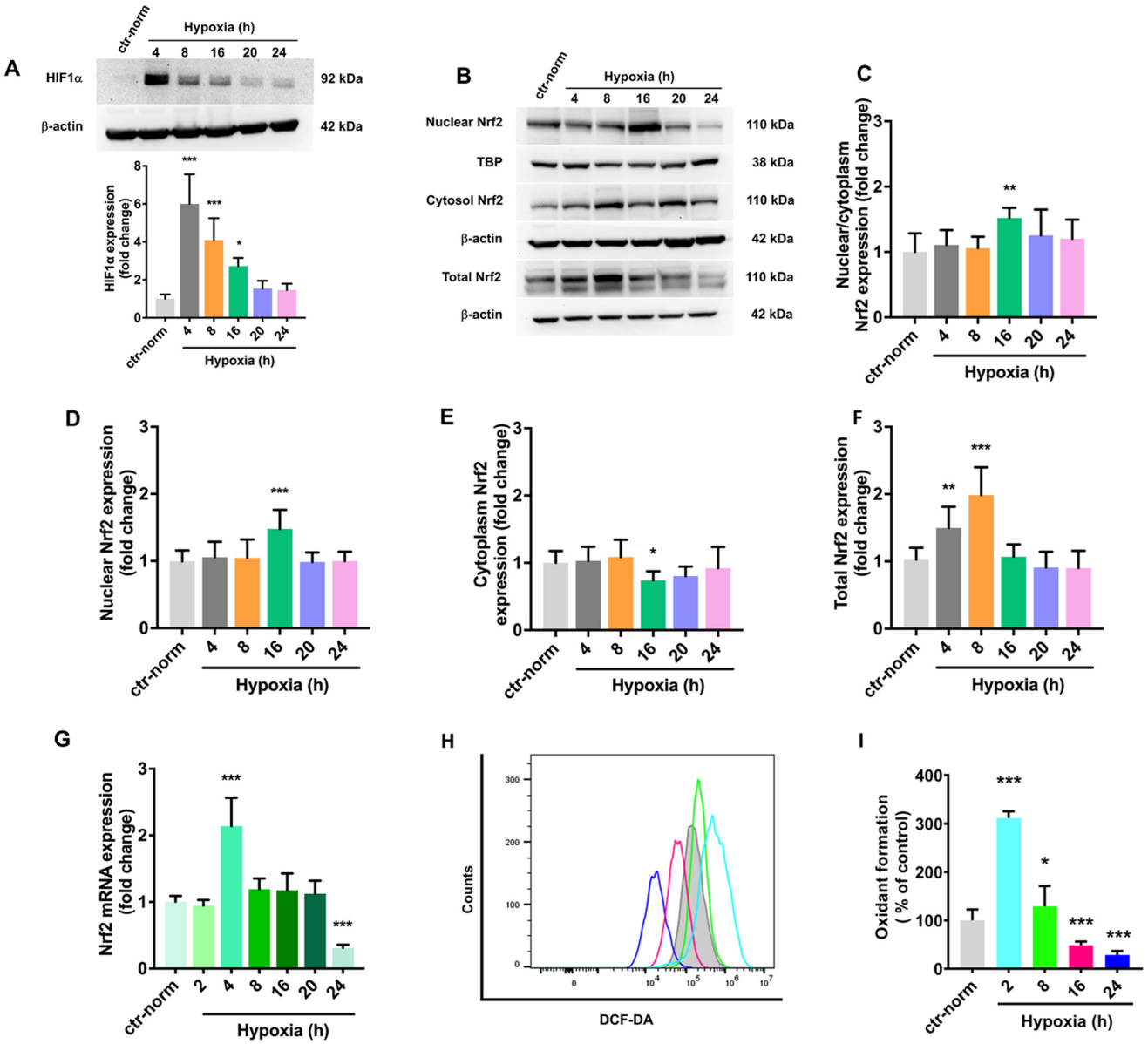

Figure 2. Hypoxia induces HIF-1α and activates Nrf2 signaling in U87MG cells. U87MG cells were exposed to hypoxia (1% O_2) for the indicated durations. (A) Representative immunoblots and quantification of HIF-1α. Nrf2 nuclear accumulation was assessed by fractionation followed by immunoblotting: (B) representative blots and quantification of (C) the N/C Nrf2 ratio, (D) nuclear Nrf2, (E) cytosolic Nrf2 and (F) total Nrf2. For Nrf2 immunoblots, quantification was restricted to the band in the expected molecular-weight region (100-130 kDa); lower-molecular-weight nonspecific bands were not quantified. (G) Nrf2 mRNA expression measured by qPCR. (H) Intracellular ROS measured by DCFH-DA staining and flow cytometry and (I) the corresponding quantification expressed as a percentage of the normoxic control. Data are presented as the mean ± SD (n≥3). Statistical significance was determined by one-way ANOVA followed by Dunnett's post hoc test. *P<0.05, **P<0.01 and ***P<0.001 vs. normoxia. HIF-1α, hypoxia-inducible factor 1 alpha; Nrf2, nuclear factor erythroid 2-related factor 2; N/C, nuclear/cytosolic; qPCR, quantitative polymerase chain reaction; ROS, reactive oxygen species; DCFH-DA, 2',7'-dichlorodihydrofluorescein diacetate; ctr-norm, normoxic control.

antioxidant- and stress-related gene expression compared with TMZ alone (Fig. S3). GCLM, GPX, GST, HO-1, NQO1, SOD1, NF-κB, TGF-β, EGF and EGFR showed only minor variation between the two treatment conditions. Hypoxia also promoted EGFR activation, with the p-EGFR/EGFR ratio peaking 8 h after exposure (P=0.015; Fig. 4C). Co-treatment with TMZ and brusatol markedly attenuated hypoxia-induced EGFR phosphorylation compared with TMZ alone (P=0.030; Fig. 4D). These findings indicated that suppression of Nrf2 pathway output is associated with reduced antioxidant gene expression and EGFR signaling during TMZ sensitization under hypoxia.

Brusatol-associated TMZ sensitization is accompanied by attenuation of the hypoxia-induced PGC-1α axis and increased oxidative DNA damage. To examine the PGC-1α signaling axis, U87MG cells were treated with TMZ, brusatol, or their combination under hypoxia for 24 h. Immunofluorescence analysis showed that hypoxia increased the nuclear-to-cytoplasmic PGC-1α fluorescence intensity ratio (P<0.001; Fig. 5A and B), nuclear PGC-1α fluorescence intensity (P=0.010; Fig. 5C) and whole-cell PGC-1α fluorescence intensity (P<0.01; Fig. 5E). Co-treatment with TMZ and brusatol attenuated these hypoxia-associated changes relative to TMZ alone, reducing PGC-1α nuclear localization

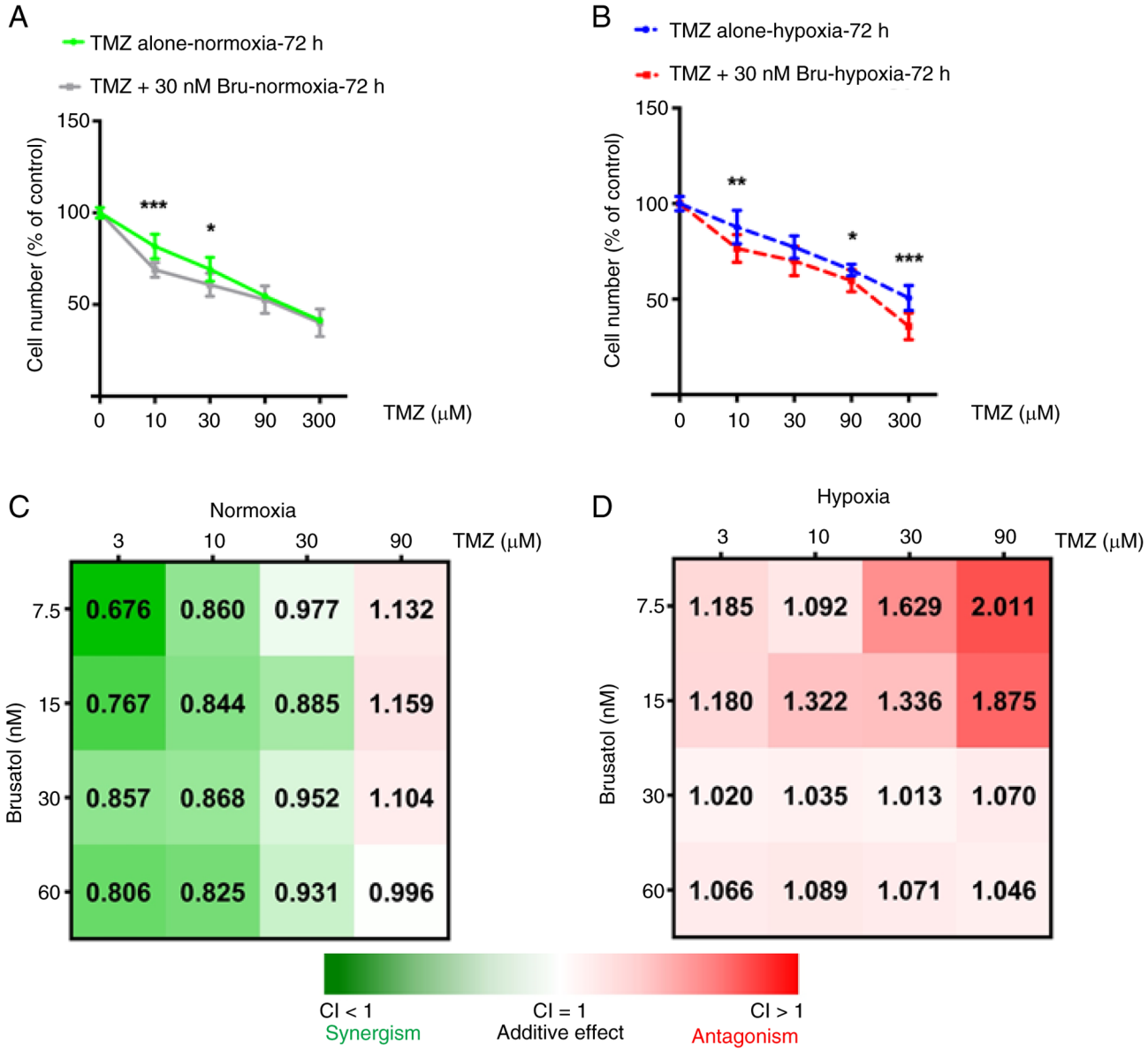

Figure 3. Bru enhances TMZ sensitivity in U87MG cells under conditions associated with suppression of Nrf2 pathway output. U87MG cells were treated with TMZ (0-300 μM) with or without Bru (30 nM) for 72 h under normoxia or hypoxia, and relative cell number was assessed by DAPI-based cell counting. Dose-response curves were generated under (A) normoxia and (B) hypoxia. Values are expressed as percentages of the corresponding 0 μM TMZ condition within each curve; thus, each TMZ dose-response curve was normalized to its own baseline (100%). At matched TMZ concentrations, TMZ alone and TMZ plus Bru were compared using unpaired two-tailed Student's t-test. *P<0.05, **P<0.01, and ***P<0.001 vs. TMZ at the same concentration without Bru. Heat maps show the CI for TMZ-brusatol combinations under (C) normoxia and (D) hypoxia. CI<1, CI=1 and CI>1 indicate synergism, additivity and antagonism, respectively. Bru, brusatol; TMZ, temozolomide; Nrf2, nuclear factor erythroid 2-related factor 2; CI, combination index.

and overall fluorescence intensity. Under normoxia, the TMZ-alone and combination groups showed broadly similar PGC-1α localization and fluorescence patterns (Fig. S4). The present study next examined PGC-1α mRNA and downstream mitochondrial genes (Fig. 5F-I). Hypoxia markedly increased PGC-1α mRNA expression (P<0.001; Fig. 5F), as well as the expression of SIRT3 (P<0.001; Fig. 5G), CYCS (P<0.001; Fig. 5H), and ATP5F1B (P<0.001; Fig. 5I) compared with the normoxic control. Co-treatment with TMZ and brusatol reduced the hypoxia-induced expression of PGC-1α and these downstream genes relative to TMZ alone. The corresponding normoxic expression profiles are shown in Fig. S5. Oxidative DNA damage, assessed using 8-OHdG, was higher in the TMZ-plus-brusatol group than in the TMZ-alone group under hypoxia (Fig. 5J and K). Under normoxia, combination treatment did not produce an evident increase in 8-OHdG fluorescence relative to TMZ alone (Fig. S6). Together, these findings show that brusatol-associated TMZ sensitization under hypoxia is accompanied by attenuation of PGC-1α-associated mitochondrial responses and increased oxidative DNA damage.

Discussion

Hypoxia contributes to cancer progression and chemoresistance by engaging coordinated cellular stress-response programs (15,35). HIF-1α is a central regulator of hypoxic adaptation and orchestrates transcriptional networks that

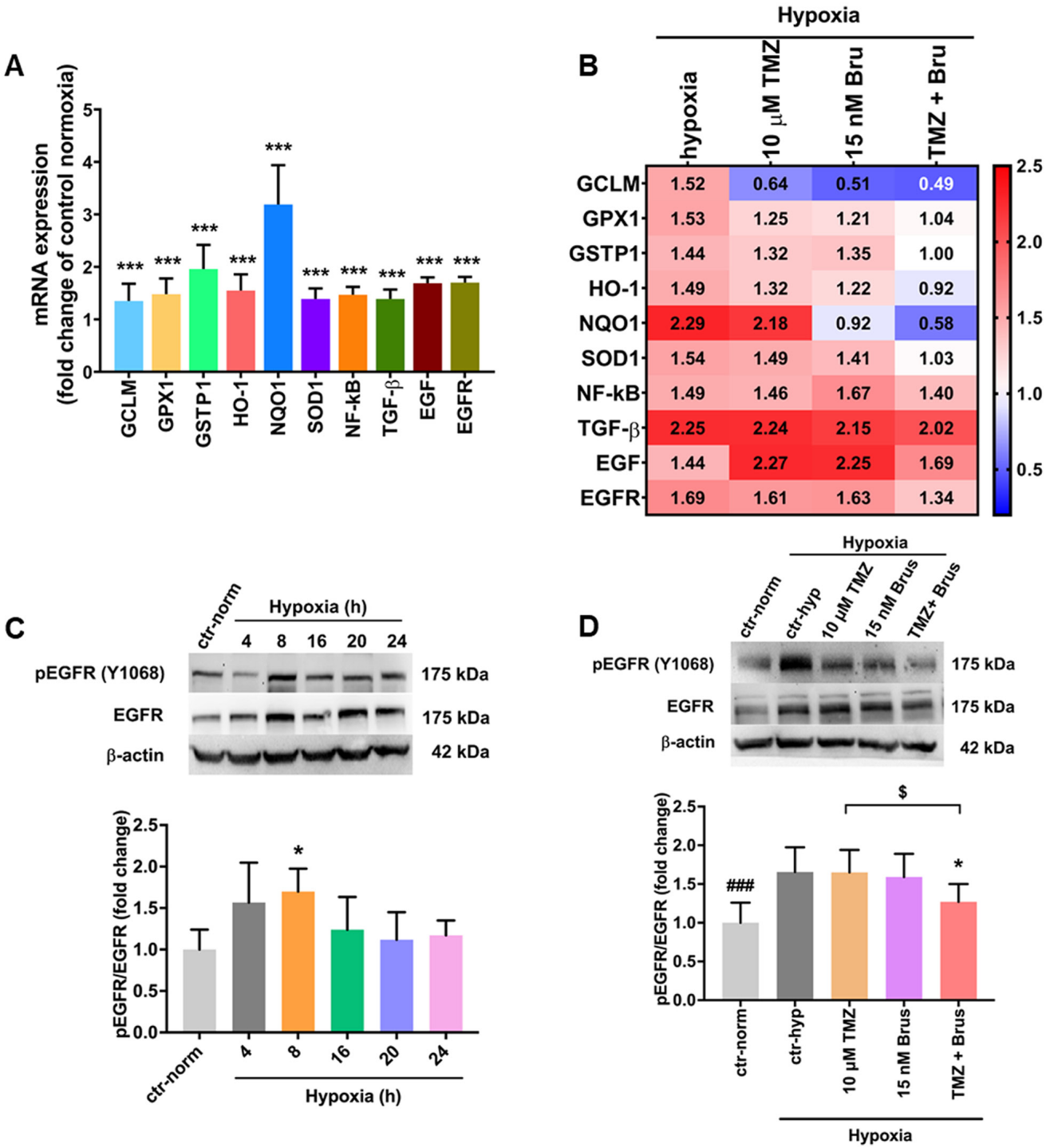

Figure 4. Hypoxia induces antioxidant and growth factor-related gene expression and activates EGFR signaling in U87MG cells. U87MG cells were exposed to normoxia or hypoxia (1% O^2) and treated with TMZ and/or Bru as indicated. (A) mRNA expression of antioxidant and growth factor-related signaling genes under normoxia and hypoxia, measured by qPCR. (B) Heat map of gene-expression changes in hypoxic cells treated with TMZ and/or Bru. (C) Representative immunoblots and quantification of the p-EGFR/EGFR ratio under normoxia and hypoxia. (D) Representative immunoblots and quantification of the p-EGFR/EGFR ratio in hypoxic cells treated with TMZ and/or Bru. Data are presented as the mean ± SD (n≥3). Comparisons between normoxic and hypoxic controls and between TMZ-alone and combination treatment groups were performed using an unpaired two-tailed Student's t-test (***P<0.001, $^{###}$P<0.001, and $^{\$}$P<0.05, as indicated). Comparisons among multiple treatment groups were analyzed using one-way ANOVA followed by Dunnett's post hoc test (*P<0.05 vs. the hypoxic control). EGFR, epidermal growth factor receptor; TMZ, temozolomide; Bru, brusatol; qPCR, quantitative polymerase chain reaction; p-, phosphorylated.

promote tumor growth, invasion, and metabolic reprogramming (36,37). In parallel, Nrf2 provides cytoprotection against oxidative and environmental stressors and has been implicated in hypoxia-associated drug resistance across solid tumors (18,38). Elevated Nrf2 activity is associated with poor outcomes in several cancers and has been proposed as a therapeutic target for overcoming chemoresistance. Studies have highlighted Nrf2-targeted strategies as a promising

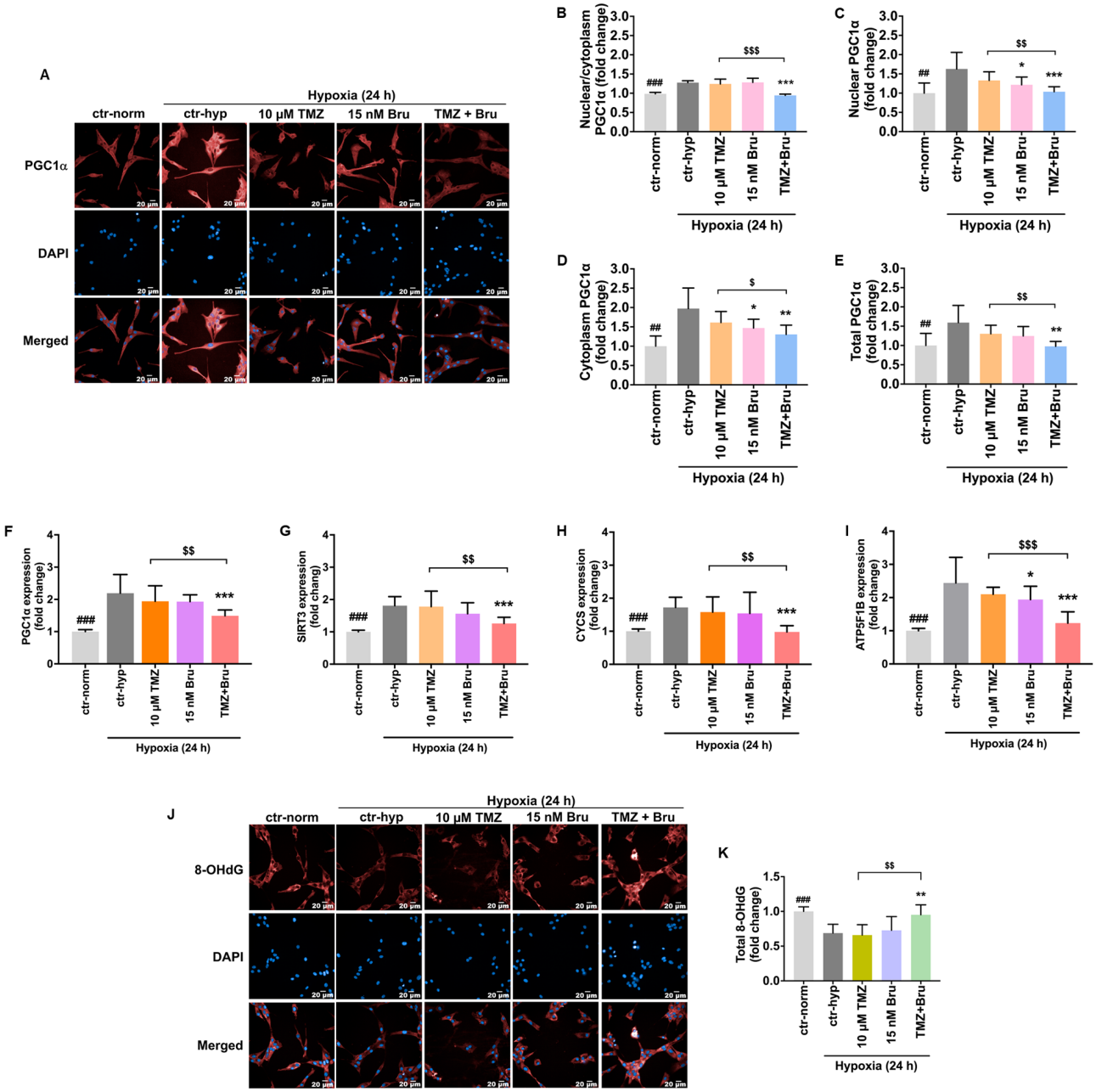

Figure 5. Bru-associated TMZ sensitization is accompanied by attenuation of the hypoxia-induced PGC-1α axis and increased oxidative DNA damage in U87MG cells. U87MG cells were treated with TMZ and/or Bru under hypoxia (1% O_2) for 24 h. Immunofluorescence analysis of PGC-1α expression and nuclear localization. (A) Representative images of PGC-1α (Alexa Fluor 647) and nuclei (DAPI). Quantification includes (B) the nuclear-to-cytoplasmic fluorescence intensity ratio and (C) nuclear, (D) cytoplasmic and (E) whole-cell mean PGC-1α fluorescence intensities. Expression of (F) PGC-1α and the downstream mitochondrial genes (G) SIRT3, (H) CYCS and (I) ATP5F1B, measured by qPCR. Oxidative DNA damage assessed by 8-OHdG staining: (J) Representative images (magnification, x40) and (K) quantification of whole-cell mean 8-OHdG intensity. Data are presented as the mean ± SD (n≥3). Comparisons between normoxic and hypoxic controls and between TMZ-alone and combination treatment groups were performed using an unpaired two-tailed Student's t-test ($^{\#\#}$P<0.01 $^{\#\#\#}$P<0.001 and $^{\$}$P<0.05, $^{\$\$}$P<0.01, $^{\$\$\$}$P<0.001 respectively). Comparisons among multiple treatment groups were analyzed using one-way ANOVA followed by Dunnett's post hoc test (*P<0.05, **P<0.01, and ***P<0.001 vs. the hypoxic control). Bru, brusatol; TMZ, temozolomide; PGC-1α, peroxisome proliferator-activated receptor gamma coactivator 1 alpha; 8-OHdG, 8-hydroxy-2'-deoxyguanosine; SIRT3, sirtuin 3; CYCS, cytochrome *c*; ATP5F1B, ATP synthase F1 subunit β; qPCR, quantitative polymerase chain reaction; ctr-norm, normoxic control; ctr-hyp, hypoxic control.

preclinical approach, including small-molecule Nrf2 inhibitors that may enhance responses to chemotherapy and targeted therapies, partly by increasing oxidative stress and promoting ferroptotic cell death (18,39-41). However, most Nrf2-directed strategies remain at the preclinical stage, and further optimization of selectivity, pharmacokinetic properties and safety is needed before clinical application. In the present study, hypoxia reduced TMZ sensitivity in U87MG cells and was accompanied by increased HIF-1α expression, Nrf2 nuclear accumulation, Nrf2 mRNA expression, and Nrf2 target gene induction. ROS increased transiently at 2 h and then decreased at 8-16 h. The later decrease should not be interpreted as evidence of Nrf2-dependent antioxidant control alone, because oxygen limitation can also reduce mitochondrial

electron transport and OXPHOS-dependent ROS generation. Nrf2-driven antioxidant programs may further buffer residual oxidative stress, but the present data did not distinguish reduced ROS production from increased ROS detoxification. Thus, the ROS time course was interpreted as hypoxia-associated redox remodeling that occurs in parallel with Nrf2 signaling, rather than as direct evidence of a Nrf2-dependent mechanism. Brusatol has been reported to sensitize several cancer models to chemotherapy, including GBM, breast cancer and lung adenocarcinoma models (21,31,42,43). Although brusatol was initially described as reducing Nrf2 protein abundance and Nrf2-dependent transcription, subsequent studies identified broader post-transcriptional effects, including inhibition of protein translation. Brusatol is therefore best interpreted as a pharmacological suppressor of Nrf2 pathway output with known off-target liabilities, most notably its broad inhibition of protein translation, which can transiently deplete other short-lived proteins such as HIF-1α. In the present study, brusatol had little effect on baseline cell number under hypoxia but enhanced TMZ-associated loss of cell number. This pattern is consistent with a role for stress-response defenses during treatment exposure, but it does not establish that the effect is exclusively Nrf2 dependent. Nrf2 dependence under hypoxia is model- and paradigm-dependent and studies showing Nrf2-dependent survival have often used genetic Nrf2 loss and/or more severe or prolonged oxygen stress, including hypoxia-reoxygenation (16,17,44). Hypoxia also activates redundant pro-survival pathways, including HIF-1α, EGFR-PI3K/AKT, NF-κB and TGF-β signaling, that may preserve viability despite partial suppression of Nrf2 pathway output.

A further mechanistic consideration is that brusatol, as a global inhibitor of protein translation, is expected to deplete not only Nrf2 but also other short-lived, translation-dependent transcription factors, including HIF-1α. Under hypoxia, HIF-1α abundance depends on continuous *de novo* synthesis balanced against oxygen-dependent degradation, rendering it particularly sensitive to translational blockade; consistent with this, brusatol has been reported to reduce HIF-1α protein and to suppress HIF-1 target-gene output under hypoxic conditions (45). Several readouts affected by brusatol in the present study are regulated, at least in part, by HIF-1α: Hypoxic reinforcement of EGFR and EGFR-PI3K/AKT signaling is HIF-associated (4,8,34) and the hypoxic transcriptional reprogramming that shapes redox balance and metabolic adaptation is coordinated by HIF-1α acting together with other stress-response regulators. As HIF-1α and Nrf2 signaling are interconnected and both depend on ongoing translation, the brusatol-associated reductions in antioxidant and growth factor-related gene expression, EGFR phosphorylation and PGC-1α-linked mitochondrial gene expression, together with the increase in oxidative DNA damage, cannot be attributed exclusively to suppression of Nrf2 pathway output; these effects may also involve suppression of HIF-1α-dependent pathways. They are therefore more accurately interpreted as reflecting brusatol-mediated suppression of a broader hypoxia-adaptive network encompassing both HIF-1α- and Nrf2-dependent programs. Notably, HIF-1α induction in this model was transient, peaking at 4 h and declining by 20-24 h, whereas the combination experiments were performed at 24 h; this temporal profile may limit, although it does not exclude, a HIF-1α-dependent contribution. Direct measurement of HIF-1α protein and canonical HIF-1 target genes (such as VEGFA, SLC2A1/GLUT1, CA9) after brusatol treatment under hypoxia, particularly in the TMZ and TMZ-plus-brusatol conditions, will be required to delineate the relative contributions of HIF-1α- and Nrf2-dependent signaling to the observed TMZ sensitization.

Hypoxia increased antioxidant and growth factor-related gene expression and enhanced EGFR phosphorylation. Brusatol-associated suppression of Nrf2 pathway output was accompanied by reduced antioxidant gene expression and lower EGFR phosphorylation. ROS can function as a secondary messenger in EGFR signaling, and previous studies have linked Nrf2 and EGFR activation to therapy resistance (46-51). The present data therefore supported an association among redox adaptation, EGFR signaling and TMZ sensitivity under hypoxia. However, because brusatol has broad effects and no pathway-specific rescue experiment was performed, the data did not demonstrate that Nrf2 directly regulates EGFR phosphorylation in this model.

The findings also suggested an association between hypoxic stress adaptation and mitochondrial remodeling. Hypoxia increased PGC-1α nuclear localization and fluorescence intensity and upregulated PGC-1α-associated mitochondrial genes. Co-treatment with TMZ and brusatol attenuated these responses and increased 8-OHdG fluorescence. Persistent Nrf2 signaling has been linked to the maintenance of mitochondrial integrity and cooperation with PGC-1α-associated programs that support tumor survival and therapy tolerance (20,52). In the present study, however, PGC-1α activity was not measured directly; the conclusions are based on subcellular localization, fluorescence intensity and mRNA expression. The relationship may involve direct Nrf2-PGC-1α crosstalk or indirect regulation through altered redox and energetic signaling, and dedicated mechanistic studies will be required to distinguish these possibilities.

The translational implications of these findings should be considered cautiously. First, brusatol is not a selective Nrf2 inhibitor; as a global inhibitor of protein translation it broadly depletes short-lived proteins, and the observed responses therefore cannot be attributed exclusively to suppression of Nrf2 pathway output. In particular, HIF-1α is itself a labile, translation-dependent transcription factor and brusatol has been shown to reduce HIF-1α protein and HIF-1 target-gene expression under hypoxia (45). As HIF-1α was not measured after brusatol treatment in the present model and because several of the pathways examined here, including EGFR signaling and the PGC-1α-linked mitochondrial program, are influenced by HIF-1α, the effects observed with brusatol may reflect suppression of HIF-1α-dependent pathways in addition to Nrf2 pathway output. Direct assessment of HIF-1α protein and downstream hypoxia-response markers following brusatol treatment, particularly under TMZ and TMZ-plus-brusatol conditions, is needed to resolve these contributions. Second, the observed associations among Nrf2, EGFR signaling and PGC-1α do not establish causality. Genetic manipulation, pathway-specific inhibition and rescue experiments are required to clarify the underlying mechanisms. Third, mechanistic analyses were limited to U87MG cells because

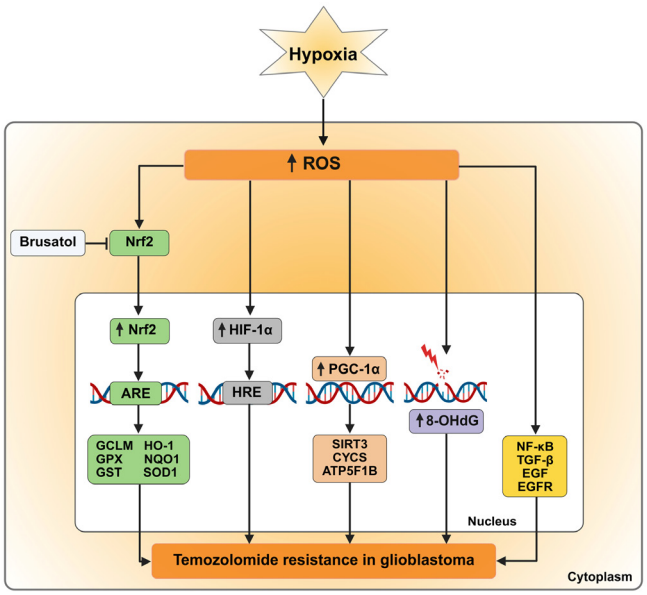

Figure 6. Proposed model of hypoxia-associated Nrf2 and PGC-1α signaling in temozolomide resistance in glioblastoma. Under hypoxia, U87MG glioblastoma cells show increased nuclear accumulation of Nrf2 and HIF-1α, which engage ARE and HRE, respectively. This drives upregulation of antioxidant and cytoprotective genes, including GCLM, HO-1, NQO1, and SOD1, as well as members of the GPX and GST gene families, together with growth- and survival-related genes (NF-κB, EGF, TGF-β, and EGFR), and a PGC-1α-associated mitochondrial transcriptional program (including SIRT3 and ATP5F1B), while limiting oxidative DNA damage (8-OHdG), collectively contributing to temozolomide resistance. Pharmacological suppression of Nrf2 pathway output with brusatol attenuates these hypoxia-adaptive responses, reducing antioxidant and growth factor-related gene expression and PGC-1α-linked mitochondrial responses while increasing oxidative DNA damage, thereby enhancing temozolomide sensitivity under hypoxic conditions. Nrf2, nuclear factor erythroid 2-related factor 2; PGC-1α, peroxisome proliferator-activated receptor gamma coactivator 1 alpha; HIF-1α, hypoxia-inducible factor 1 alpha; ARE, antioxidant response elements; HRE, hypoxia response elements; GCLM, glutamate-cysteine ligase modifier subunit; HO-1, heme oxygenase 1; GPX, glutathione peroxidase; NQO1, NAD(P)H quinone oxidoreductase 1; GST, glutathione S-transferase; SOD1, superoxide dismutase 1; NF-κB, nuclear factor kappa B; EGF, epidermal growth factor; TGF-β, transforming growth factor beta; EGFR, epidermal growth factor receptor; SIRT3, sirtuin 3; ATP5F1B, ATP synthase F1 subunit beta; 8-OHdG, 8-hydroxy-2'-deoxyguanosine; ROS, reactive oxygen species.

U138MG cells did not show a hypoxia-dependent shift in treatment response; consequently, generalizability to other GBM subtypes remains uncertain. Fourth, the simplified *in vitro* model (1% O_2) does not reproduce the cellular complexity or oxygen heterogeneity of the tumor microenvironment. Finally, the absence of *in vivo* validation limits clinical extrapolation, and blood-brain barrier penetration remains a major challenge for Nrf2-targeted therapies. Studies using patient-derived cells, three-dimensional models, and orthotopic animal models are needed to validate the findings and assess their translational relevance.

In summary, hypoxia reduced TMZ sensitivity in U87MG cells, whereas co-treatment with TMZ and brusatol enhanced TMZ sensitivity under these conditions (Fig. 6). This sensitization was associated with reduced antioxidant gene expression, lower EGFR phosphorylation, attenuation of PGC-1α-associated mitochondrial responses and increased oxidative DNA damage. The differential responses of U87MG and U138MG cells underscore the model dependence of hypoxia-associated TMZ resistance and limit generalizability. As brusatol is not a selective Nrf2 inhibitor but a global translation inhibitor and because the study did not include direct genetic validation of Nrf2 or measurement of HIF-1α responses to brusatol under hypoxia, the observed effects may reflect suppression of HIF-1α-dependent pathways in addition to Nrf2 pathway output; the findings therefore support an association rather than definitive Nrf2-dependent causality. Further studies using orthogonal Nrf2-targeting approaches, direct evaluation of HIF-1α pathway responses, additional GBM models, and *in vivo* systems are needed to define the underlying mechanisms and translational relevance more clearly.

Acknowledgements

Not applicable.

Funding

The present study was supported by Siriraj Research and Development Fund Type II (grant no. R016233001), Faculty of Medicine Siriraj Hospital, Mahidol University, Thailand.

Availability of data and materials

The data generated in the present study may be requested from the corresponding author.

Authors' contributions

PT, SJ, SS and UP conceived the study. TO and SP designed and performed the experiments. TO, SP and UP performed the data analysis. TO and UP prepared the original draft and constructed figures. PT, SJ, SS and UP reviewed and edited the manuscript. UP supervised the study and was responsible for project administration and funding acquisition. TO and UP confirm the authenticity of all the raw data. All authors read and approved the final manuscript.

Ethics approval and consent to participate

Not applicable.

Patient consent for publication

Not applicable.

Competing interests

The authors declare that they have no competing interests.

Use of artificial intelligence tools

During the preparation of this work, artificial intelligence tools were used to improve the readability and language of the manuscript or to generate images, and subsequently, the authors revised and edited the content produced by the artificial intelligence tools as necessary, taking full responsibility for the ultimate content of the present manuscript.

References

1. Tan AC, Ashley DM, López GY, Malinzak M, Friedman HS and Khasraw M: Management of glioblastoma: State of the art and future directions. CA Cancer J Clin 70: 299-312, 2020.
2. Sousa N, Geiß C, Bindila L, Lieberwirth I, Kim E and Régnier-Vigouroux A: Targeting sphingolipid metabolism with the sphingosine kinase inhibitor SKI-II overcomes hypoxia-induced chemotherapy resistance in glioblastoma cells: Effects on cell death, self-renewal, and invasion. BMC Cancer 23: 762, 2023.
3. Thakur A, Faujdar C, Sharma R, Sharma S, Malik B, Nepali K and Liou JP: Glioblastoma: Current status, emerging targets, and recent advances. J Med Chem 65: 8596-8685, 2022.
4. Monteiro AR, Hill R, Pilkington GJ and Madureira PA: The role of hypoxia in glioblastoma invasion. Cells 6: 45, 2017.
5. Walsh JC, Lebedev A, Aten E, Madsen K, Marciano L and Kolb HC: The clinical importance of assessing tumor hypoxia: Relationship of tumor hypoxia to prognosis and therapeutic opportunities. Antioxid Redox Signal 21: 1516-1554, 2014.
6. Ge X, Pan MH, Wang L, Li W, Jiang C, He J, Abouzid K, Liu LZ, Shi Z and Jiang BH: Hypoxia-mediated mitochondria apoptosis inhibition induces temozolomide treatment resistance through miR-26a/Bad/Bax axis. Cell Death Dis 9: 1128, 2018.
7. Singh N, Miner A, Hennis L and Mittal S: Mechanisms of temozolomide resistance in glioblastoma-a comprehensive review. Cancer Drug Resist 4: 17-43, 2021.
8. Mao XG, Xue XY, Lv R, Ji A, Shi TY, Chen XY, Jiang XF and Zhang X: CEBPD is a master transcriptional factor for hypoxia regulated proteins in glioblastoma and augments hypoxia induced invasion through extracellular matrix-integrin mediated EGFR/PI3K pathway. Cell Death Dis 14: 269, 2023.
9. Chandel NS, McClintock DS, Feliciano CE, Wood TM, Melendez JA, Rodriguez AM and Schumacker PT: Reactive oxygen species generated at mitochondrial complex III stabilize hypoxia-inducible factor-1alpha during hypoxia: A mechanism of O2 sensing. J Biol Chem 275: 25130-25138, 2000.
10. Schroedl C, McClintock DS, Budinger GRS and Chandel NS: Hypoxic but not anoxic stabilization of HIF-1alpha requires mitochondrial reactive oxygen species. Am J Physiol Lung Cell Mol Physiol 283: L922-L931, 2002.
11. Guzy RD, Hoyos B, Robin E, Chen H, Liu L, Mansfield KD, Simon MC, Hammerling U and Schumacker PT: Mitochondrial complex III is required for hypoxia-induced ROS production and cellular oxygen sensing. Cell Metab 1: 401-408, 2005.
12. Masson N, Willam C, Maxwell PH, Pugh CW and Ratcliffe PJ: Independent function of two destruction domains in hypoxia-inducible factor-alpha chains activated by prolyl hydroxylation. EMBO J 20: 5197-5206, 2001.
13. Chan DA, Sutphin PD, Yen SE and Giaccia AJ: Coordinate regulation of the oxygen-dependent degradation domains of hypoxia-inducible factor 1 alpha. Mol Cell Biol 25: 6415-6426, 2005.
14. Kobayashi A, Kang MI, Okawa H, Ohtsuji M, Zenke Y, Chiba T, Igarashi K and Yamamoto M: Oxidative stress sensor Keap1 functions as an adaptor for Cul3-based E3 ligase to regulate proteasomal degradation of Nrf2. Mol Cell Biol 24: 7130-7139, 2004.
15. Bae T, Hallis SP and Kwak MK: Hypoxia, oxidative stress, and the interplay of HIFs and NRF2 signaling in cancer. Exp Mol Med 56: 501-514, 2024.
16. Ji X, Wang H, Zhu J, Zhu L, Pan H, Li W, Zhou Y, Cong Z, Yan F and Chen S: Knockdown of Nrf2 suppresses glioblastoma angiogenesis by inhibiting hypoxia-induced activation of HIF-1α. Int J Cancer 135: 574-584, 2014.
17. Tang T, Jia Y, Liang H, Han Y, Cong Z, Wang H and Ji X: Knockdown of Nrf2 radiosensitizes glioma cells by inducing redox stress and apoptosis in hypoxia. Transl Cancer Res 11: 4105-4116, 2022.
18. Wang XJ, Sun Z, Villeneuve NF, Zhang S, Zhao F, Li Y, Chen W, Yi X, Zheng W, Wondrak GT, *et al*: Nrf2 enhances resistance of cancer cells to chemotherapeutic drugs, the dark side of Nrf2. Carcinogenesis 29: 1235-1243, 2008.
19. Tan Z, Luo X, Xiao L, Tang M, Bode AM, Dong Z and Cao Y: The role of PGC1α in cancer metabolism and its therapeutic implications. Mol Cancer Ther 15: 774-782, 2016.
20. Luchkova A, Mata A and Cadenas S: Nrf2 as a regulator of energy metabolism and mitochondrial function. FEBS Lett 598: 2092-2105, 2024.
21. Ren D, Villeneuve NF, Jiang T, Wu T, Lau A, Toppin HA and Zhang DD: Brusatol enhances the efficacy of chemotherapy by inhibiting the Nrf2-mediated defense mechanism. Proc Natl Acad Sci USA 108: 1433-1438, 2011.
22. Harder B, Tian W, La Clair JJ, Tan AC, Ooi A, Chapman E and Zhang DD: Brusatol overcomes chemoresistance through inhibition of protein translation. Mol Carcinog 56: 1493-1500, 2017.
23. Olayanju A, Copple IM, Bryan HK, Edge GT, Sison RL, Wong MW, Lai ZQ, Lin ZX, Dunn K, Sanderson CM, *et al*: Brusatol provokes a rapid and transient inhibition of Nrf2 signaling and sensitizes mammalian cells to chemical toxicity-implications for therapeutic targeting of Nrf2. Free Radic Biol Med 78: 202-212, 2015.
24. Shankar A, Jain M, Lim MJ, Angara K, Zeng P, Arbab SA, Iskander A, Ara R, Arbab AS and Achyut BR: Anti-VEGFR2 driven nuclear translocation of VEGFR2 and acquired malignant hallmarks are mutation dependent in glioblastoma. J Cancer Sci Ther 8: 172-178, 2016.
25. Suppramote O, Prasopporn S, Aroonpruksakul S, Ponvilawan B, Makjaroen J, Suntiparpluacha M, Korphaisarn K, Charngkaew K, Chanwat R, Pisitkun T, *et al*: The acquired vulnerability caused by CDK4/6 inhibition promotes drug synergism between oxaliplatin and palbociclib in cholangiocarcinoma. Front Oncol 12: 877194, 2022.
26. Lohakul J, Chaiprasongsuk A, Jeayeng S, Saelim M, Muanjumpon P, Thanachaiphiwat S, Tripatara P, Soontrapa K, Lumlerdkij N, Akarasereenont P and Panich U: The protective effect of polyherbal formulation, harak formula, on UVA-induced photoaging of human dermal fibroblasts and mouse skin via promoting Nrf2-regulated antioxidant defense. Front Pharmacol 12: 649820, 2021.
27. Livak KJ and Schmittgen TD: Analysis of relative gene expression data using real-time quantitative PCR and the 2(-Delta Delta C(T)) method. Methods 25: 402-408, 2001.
28. Chaiprasongsuk A, Onkoksoong T, Pluemsamran T, Limsaengurai S and Panich U: Photoprotection by dietary phenolics against melanogenesis induced by UVA through Nrf2-dependent antioxidant responses. Redox Biol 8: 79-90, 2016.
29. Htut NW, Onkoksoong T, Saelim M, Kueanjinda P, Sampattavanich S and Panich U: Live-cell imaging Unveils stimulus-specific dynamics of Nrf2 activation in UV-exposed melanoma cells: Implications for antioxidant compound screening. Free Radic Biol Med 211: 1-11, 2024.
30. Arfin S, Jha NK, Jha SK, Kesari KK, Ruokolainen J, Roychoudhury S, Rathi B and Kumar D: Oxidative stress in cancer cell metabolism. Antioxidants (Basel) 10: 642, 2021.
31. Dai Z, Cai L, Chen Y, Wang S, Zhang Q, Wang C, Tu M, Zhu Z, Li Q and Lu X: Brusatol inhibits proliferation and invasion of glioblastoma by down-regulating the expression of ECM1. Front Pharmacol 12: 775680, 2021.
32. Gao Y, Zhang E, Liu B, Zhou K, He S, Feng L, Wu G, Cao M, Wu H, Cui Y, *et al*: Integrated analysis identified core signal pathways and hypoxic characteristics of human glioblastoma. J Cell Mol Med 23: 6228-6237, 2019.
33. Culver C, Sundqvist A, Mudie S, Melvin A, Xirodimas D and Rocha S: Mechanism of hypoxia-induced NF-kappaB. Mol Cell Biol 30: 4901-4921, 2010.
34. Wang P, Zhao L, Gong S, Xiong S, Wang J, Zou D, Pan J, Deng Y, Yan Q, Wu N and Liao B: HIF1α/HIF2α-Sox2/Klf4 promotes the malignant progression of glioblastoma via the EGFR-PI3K/AKT signalling pathway with positive feedback under hypoxia. Cell Death Dis 12: 312, 2021.
35. Luo Z, Tian M, Yang G, Tan Q, Chen Y, Li G, Zhang Q, Li Y, Wan P and Wu J: Hypoxia signaling in human health and diseases: Implications and prospects for therapeutics. Signal Transduc Target Ther 7: 218, 2022.
36. Unwith S, Zhao H, Hennah L and Ma D: The potential role of HIF on tumour progression and dissemination. Int J Cancer 136: 2491-2503, 2015.
37. Lv X, Li J, Zhang C, Hu T, Li S, He S, Yan H, Tan Y, Lei M, Wen M and Zuo J: The role of hypoxia-inducible factors in tumor angiogenesis and cell metabolism. Genes Dis 4: 19-24, 2016.
38. Awuah WA, Toufik A-R, Yarlagadda R, Mikhailova T, Mehta A, Huang H, Kundu M, Lopes L, Benson S, Mykola L, *et al*: Exploring the role of Nrf2 signaling in glioblastoma multiforme. Discov Oncol 13: 94, 2022.
39. Adinolfi S, Patinen T, Jawahar Deen A, Pitkänen S, Härkönen J, Kansanen E, Küblbeck J and Levonen AL: The KEAP1-NRF2 pathway: Targets for therapy and role in cancer. Redox Biol 63: 102726, 2023.

40. Zhang J, Xu HX, Zhu JQ, Dou YX, Xian YF and Lin ZX: Natural Nrf2 inhibitors: A review of their potential for cancer treatment. Int J Biol Sci 19: 3029-3041, 2023.
41. Harifi-Mood MS, Alemzadeh E, Barati D, Dehghani AH, Siroosi FZ, Aschner M, Samini F, Samarghandian S and Farkhondeh T: The role of Nrf2 in glioma: Therapeutic targeting strategies. Curr Cancer Drug Targets: February 14, 2025 (Epub ahead of print).
42. Syu JP, Chi JT and Kung HN: Nrf2 is the key to chemotherapy resistance in MCF7 breast cancer cells under hypoxia. Oncotarget 7: 14659-14672, 2016.
43. He T, Zhou F, Su A, Zhang Y, Xing Z, Mi L, Li Z and Wu W: Brusatol: A potential sensitizing agent for cancer therapy from Brucea javanica. Biomed Pharmacother 158: 114134, 2023.
44. Kolamunne RT, Dias IHK, Vernallis AB, Grant MM and Griffiths HR: Nrf2 activation supports cell survival during hypoxia and hypoxia/reoxygenation in cardiomyoblasts; the roles of reactive oxygen and nitrogen species. Redox Biol 1: 418-426, 2013.
45. Lu Y, Wang B, Shi Q, Wang X, Wang D and Zhu L: Brusatol inhibits HIF-1 signaling pathway and suppresses glucose uptake under hypoxic conditions in HCT116 cells. Sci Rep 6: 39123, 2016.
46. Shostak K and Chariot A: EGFR and NF-κB: Partners in cancer. Trends Mol Med 21: 385-393, 2015.
47. Zhang M, Zhang YY, Chen Y, Wang J, Wang Q and Lu H: TGF-β signaling and resistance to cancer therapy. Front Cell Dev Biol 9: 786728, 2021.
48. Uribe ML, Marrocco I and Yarden Y: EGFR in cancer: Signaling mechanisms, drugs, and acquired resistance. Cancers (Basel) 13: 2748, 2021.
49. Gong L, Yin Y, Chen C, Wan Q, Xia D, Wang M, Pu Z, Zhang B and Zou J: Characterization of EGFR-reprogrammable temozolomide-resistant cells in a model of glioblastoma. Cell Death Discov 8: 438, 2022.
50. Lee SLO, Ryu H, Son AR, Seo B, Kim J, Jung SY, Song JY, Hwang SG and Ahn J: TGF-β and hypoxia/reoxygenation promote radioresistance of A549 lung cancer cells through activation of Nrf2 and EGFR. Oxid Med Cell Longev 2016: 6823471, 2016.
51. Lim SW, Chen WC, Ko HJ, Su YF, Wu CH, Huang FL, Li CF and Tsai CY: 6-Gingerol induced apoptosis and cell cycle arrest in glioma cells via MnSOD and ERK phosphorylation modulation. Biomol Ther (Seoul) 33: 129-142, 2025.
52. Lyons A, Coleman M, Riis S, Favre C, O'Flanagan CH, Zhdanov AV, Papkovsky DB, Hursting SD and O'Connor R: Insulin-like growth factor 1 signaling is essential for mitochondrial biogenesis and mitophagy in cancer cells. J Biol Chem 292: 16983-16998, 2017.